Electric-field effects on the radiative recombination in type-II ZnSe/BeTe heterostructures with equivalent and nonequivalent interfaces

S. V. Zaitsev, A. A. Maksimov, P. S. Dorozhkin, V. D. Kulakovskii, and I. I. Tartakovskii
Institute of Solid State Physics, Russian Academy of Sciences, 142432 Chernogolovka, Russia

D. R. Yakovlev,* W. Ossau, L. Hansen, and G. Landwehr
Physikalisches Institut der Universität Würzburg, 97074 Würzburg, Germany

A. Waag
Abteilung Halbleiterphysik, Universität Ulm, 89081 Ulm, Germany

(Received 24 March 2002; revised manuscript received 1 October 2002; published 18 December 2002)

Electron-hole recombination at the interfaces formed by Zn-Te and Be-Se chemical bonds has been investigated in type-II ZnSe/BeTe heterostructures at low and high levels of excitation power by means of polarized light spectroscopy with applying of electric field across the structure. A more than fourfold variation of the matrix element squared has been reached by changing the electric field for the spatially indirect optical transitions at the interface. The radiative time of electron-hole transitions at the Se-Be interface is found to be at least 50 times longer than that at the Zn-Te interface. The contribution of Be-Se interface emission in the structures with nonequivalent (Te-Zn$\cdots$Se-Be) interfaces is negligible in the whole range of applied fields. The emission at the Te-Zn interface is carefully investigated. The ratio of matrix-elements squared along and perpendicular to the Zn-Te bonds has been found to be nearly constant in the range of carrier density $10^{11}/2\times10^{12}$ cm^{-2} and equal to 7:1.

DOI: 10.1103/PhysRevB.66.245310 PACS number(s): 79.60.Jv

I. INTRODUCTION

In type-II semiconductor heterostructures the energy minima for electrons and holes lie in different layers. Spatially separated electron and hole layers are easily realized in such systems, which greatly influences their optical properties.[1–4] One of the promising systems for both fundamental research and potential applications is a wide-gap ZnSe/BeTe semiconductor heterostructure[5,6] with a high localizing potential (>2.0 eV) for electrons in the ZnSe layer and for holes (≈ 0.9 eV), whose energy minimum lies in the BeTe layer[6,7] [Fig. 1(a)]. Such deep potential wells for carriers result in a very small penetration of the electron and hole wave functions into the neighboring layers. The radiative recombination of photoexcited electrons in the ZnSe layers and holes in BeTe layers is determined by the electron $[\Psi_e(z)]$ and hole $[\Psi_h(z)]$ wave functions overlap within a rather narrow region about 1–2 monolayers (ML) in vicinity to the type-II interface.[8] That makes the spatially indirect optical transition (IT) very sensitive to the interface properties and, in particular, to the orientation of chemical bonds at the interface.

The main specific feature of ZnSe/BeTe structure is that it contains no common atoms (NCA) at the interface. Chemical bonds across the interface in these heterostructures do not exist in either of the hosts. In the case of zinc-blende-based NCA heterostructures a variety of different interface configurations can be realized. Some of them can result in a strong in-plane optical anisotropy.[9] In the case of equivalent interface combinations, such as Te-Zn$\cdots$Zn-Te or Be-Se$\cdots$Se-Be, chemical bonds at opposite interfaces of quantum wells (QW's) lie in mutually orthogonal planes $(1\bar{1}0)$ and (110). As a result, interface contributions to the lateral anisotropy cancel each other. In NCA QW's with nonequivalent interfaces, the chemical bonds at opposite interfaces are parallel to each other. This leads to an inherent in-plane anisotropy of the optical properties.[10]

A giant lateral optical anisotropy has been proved experimentally in type-II ZnSe/BeTe heterostructures.[11,12] The emission of the spatially indirect optical transition turns out to be strongly linearly polarized along the direction $[1\bar{1}0]$ and [110], which is connected with the orientation of chemical bonds at the interfaces (a detailed analysis of the symmetrical properties of different interfaces and corresponding schemes of their chemical bonds are presented in the paper.[12]) Studies of the emission polarization anisotropy in the QW structures have shown that the polarization degree $P_l=(I_{1\bar{1}0}-I_{110})/(I_{1\bar{1}0}+I_{110})$ depends on the interface configuration and excitation power.[13] It was found that P_l as high as 75% can be observed depending on the interface configurations. However, the precise determination of the transition probabilities and matrix-element anisotropy for either Zn-Te or Be-Se transition demands the separation of the emission from a single interface. That is possible to do with the use of an external electric field applied across the type-II heterostructure. Indeed, at zero electric field the maxima of $\Psi_e(z)$ and $\Psi_h(z)$ are separated by half a multiple QW period, the electron-hole transition energies at two interfaces are equal to each other and their contributions into the luminescence signal can be hardly separated [Fig. 1(b)]. An electric field inclines the conduction and valence bands of the structure. As a result, the transition energies for the IT bands at two interfaces vary in opposite directions [Fig. 1(c)]. That allows one not only to separate the emission lines from op-

 ©2002 The American Physical Society

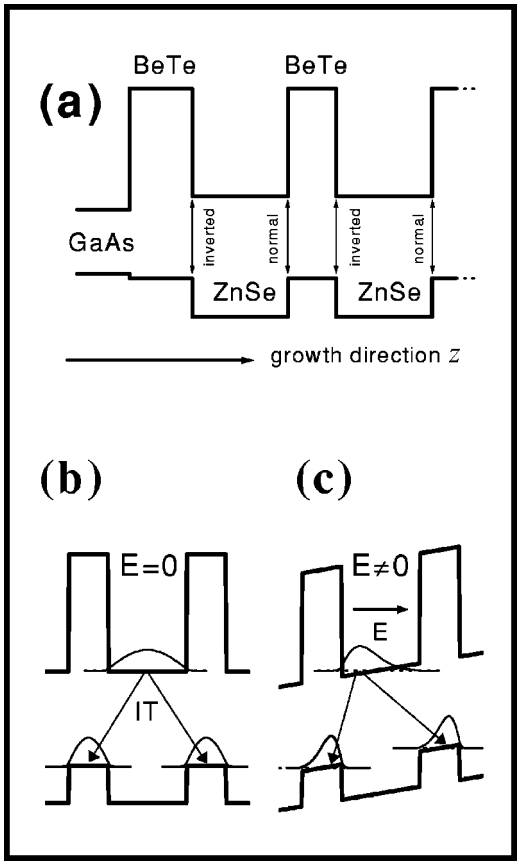

FIG. 1. Scheme of investigated ZnSe/BeTe heterostructures (a), wave functions and energy levels for electrons (in the ZnSe layer) and holes (in the BeTe layer) and spatially indirect optical transitions (IT) in structures without (b) and with applied (c) electric field.

posite interfaces but also to make the unique assignment of these transitions to either normal or inverted interface. Following the definition given in Ref. 11, in this paper the interface is referred to as a *normal* one when BeTe is growing on ZnSe and as an *inverted* one for ZnSe on BeTe case.

The objective of this paper is a comprehensive investigation of the influence of electric fields on the radiative recombination in the type-II ZnSe/BeTe heterostructures for various photoexcitation densities, a comparison of the optical matrix elements at Zn-Te and Be-Se interfaces, and the evaluation of their anisotropy.

II. EXPERIMENT

ZnSe/BeTe samples with three sets of different interface configuration were grown by molecular beam epitaxy on (001)-oriented n-doped GaAs substrates [Fig. 1(a)], namely, nonequivalent Te-Zn$\cdots$Se-Be (sample *A*), equivalent Te-Zn$\cdots$Zn-Te (sample *B*), and nonequivalent Be-Se$\cdots$Zn-Te (sample *C*) interfaces. The structures contain a five-monolayer BeTe buffer layer and five periods of alternating five-nm-thick BeTe and 10-nm-thick ZnSe layers with the last ZnSe layer as a cap.

The structure with Te-Zn$\cdots$Se-Be interfaces has at the first (inverted) interface the ZnSe layer grown on a Te-terminated BeTe layer resulting in the Te-Zn bond through the interface whereas at the second (normal) interface the BeTe layer was grown on a Se-terminated ZnSe layer resulting in the Se-Be bond. Chemical bonds at the normal and inverted interfaces are parallel to each other in samples *A* and *C* with nonequivalent interfaces, while in sample *B* with equivalent interfaces they are orthogonal to each other. Details of the termination procedure used for the growth of ZnSe/BeTe interfaces are given in Sec. II of Ref. 14. This paper also contains comprehensive information on the structural quality of the ZnSe/BeTe interfaces examined by optical microscopy, conventional and high-resolution transmission electron microscopy, x-ray diffractometry, and atomic force microscopy. It has been shown that abrupt chemical transition regions with width less than 1 ML are achieved for ZnTe-rich growth conditions. Under the BeSe-rich conditions the chemically diffuse interfaces with width of 2–3 ML's are formed.

Photoluminescence (PL) was excited by a pulsed N_2 laser with a pulse duration of 10 ns and $\lambda_{exc}=337.1$ nm (3.68 eV), with pulse repetition frequency 150 Hz. The transverse dimensions of the laser excitation spot were 0.5×0.2 mm^2. The laser emission is absorbed in the ZnSe layers with the band gap of 2.8 eV only, as the direct band gap of BeTe[15] ($\approx$4.5 eV) markedly exceeds the excitation energy. Polarized time-resolved PL spectra were recorded in the direction normal to the QW plane by use of a photomultiplier with a temporal resolution of $\sim$1 ns. At low photoexcitation densities and at low PL intensity, respectively, time-integrated PL spectra were recorded. The measurements were carried out at a temperature of 5 K.

A 5-nm-thick semitransparent Au film, deposed *in situ* on the last ZnSe layer, serves as a top electrical contact. The Schottky barrier at the Au contact to the ZnSe layer causes a built-in voltage V_{in} of -0.6 V and results in a negative electric field across the BeTe-ZnSe structure.[16] To avoid the large voltage drop on the GaAs substrates, the *n*-doped substrates have been chosen. This let us suggest that the main drop of the voltage takes place in the nondoped layers of ZnSe/BeTe heterostructures.

The range of voltages applied to the samples was limited by increasing current leading to the structure breakdown. In our samples the applied voltages were usually in the range $-0.9-+0.7$ V (the voltage *V* is referred to as positive when plus of the voltage source is connected to the gold contact). The latter is only enough to compensate V_{in}. As a result, in the largest part of the range of used biases the electric field across the structure induced by $V_{in}+V$ was negative and the carriers are shifted to the inverted interface. This situation is illustrated by Fig. 1(c). Note the inverted interface has Te-Zn bonds in the samples *A* and *B* and Be-Se bonds in the sample *C*.

III. EXPERIMENTAL RESULTS AND DISCUSSION

A. Introduction

In this section we will discuss emission spectra of a ZnSe/BeTe structure recorded in two linear polarizations. Spatially

indirect optical transitions at type II interfaces involving electrons from ZnSe layers and holes from BeTe layers will be in the center of our attention. In both polarizations there are contributions from the emission at the normal (n) and inverted (i) interfaces. Before discussing the spectra let us first describe the technique used for separation of these contributions. The emission spectrum measured in linear polarization along the $[1\bar{1}0]$ and [110] directions is $I_{1\bar{1}0(110)}(\hbar\omega)=I_{i,1\bar{1}0(110)}(\hbar\omega)+I_{n,1\bar{1}0(110)})(\hbar\omega)$. As we will show later the ratio of intensities in two polarizations $\alpha_{i(n)}=I_{i(n),1\bar{1}0}/I_{i(n),110}$ can be determined from the spectra recorded at high electric fields when the emission from the one type of interfaces dominates. In this case using $\alpha_{i(n)}$ the contributions from two interfaces can be separated as

$$I_{n,110}=(\alpha_i I_{110}-I_{1\bar{1}0})/(\alpha_i-\alpha_n), \tag{1}$$

$$I_{i,110}=(\alpha_n I_{110}-I_{1\bar{1}0})/(\alpha_n-\alpha_i). \tag{2}$$

Matrix elements for optical transitions at the interfaces for polarization along [110] ($p_{x'}$) and $[1\bar{1}0]$ ($p_{y'}$) axes can be calculated in the the tight-binding approximation.[19] Calculations show that the absolute values of $p_{x'(y')}$ depend strongly on the tunneling of electrons and holes into the neighboring layers across the type II interface but the ratio $p_{x'}/p_{y'}$ is nearly independent of electron (hole) quantization energy. Taking into account this result the transition probability can be approximated as

$$p^2_{x'(y')}\propto p^2_{0,x'(y')}J^2, \tag{3}$$

where $J^2=(\int\Psi_e\Psi_h d^3r)^2$ gives the probability to find electron and hole in one place and the term p_0^2 reflects the probability of their radiative recombination in this place. It is clear that in this approximation the change in the emission intensity at a fixed interface with electric field is determined by the variation of the electron-hole overlap, whereas the ratio of the intensities in two polarization is completely determined by the type of the interface (Te-Zn or Be-Se). In the structures with equivalent (Te-Zn$\cdots$Zn-Te or Be-Se$\cdots$Se-Be) interfaces $\alpha_i=1/\alpha_n$ due to mutually perpendicular directions of the interface layer bonds.

It is important to note that in the ZnSe/BeTe heterostructures with rather thin ($\leqslant$10 nm) ZnSe layers the hole relaxation (tunneling) time τ_{rel} from the ZnSe layer to the BeTe layer is much shorter than the radiative τ_r time of the spatial indirect transitions and nonradiative τ_{nr} time.[17] On the other hand, at low excitation powers ZnSe/BeTe heterostructures are characterized by low quantum efficiency of PL indicating that the nonradiative lifetime is much shorter than the radiative one $\tau_r\gg\tau_{nr}$. Thus, at low excitation powers the system can be characterized by an unique time τ_{nr}. In this case the measured ratio of PL intensities of spatially indirect transitions at opposite interfaces gives us the ratio of radiative recombination times at these interfaces. In turn, the change in the line intensity $I\propto\tau_r^{-1}\propto p_0^2J^2$ can be directly compared to the change in the overlap integral.

At high excitation powers quantum efficiency of PL ZnSe/BeTe heterostructures increases considerably. Figure 2 shows a typical dependence of the PL intensity on the laser excitation power P_{exc}. It is seen that at $P_{exc}\leqslant$10 kW/cm^2 the dependence of the PL intensity is linear on P_{exc}, in the region of the excitation power from $P_{exc}\approx$10 kW/cm^2 to $P_{exc}\approx$50 kW/cm^2 the PL intensity demonstrates a superlinear behavior, and at $P_{exc}\geqslant$50 kW/cm^2 the PL intensity becomes linear on P_{exc} again. As it follows from the analysis of the data represented in Fig. 2, the observed behavior of the PL intensity can be explained by an increasing saturation of the centers of nonradiative recombination at considerably increased hole concentration in the BeTe layers.[18] That in turn would cause the increase of the nonradiative τ_{nr} time, so that at high excitation powers the radiative lifetime becomes much shorter than the nonradiative one $\tau_{nr}\gg\tau_r$, and the system is characterized now by an unique time τ_r.[18] In this case the PL intensity of the spatially indirect transitions is proportional to P_{exc} and does not depend on the overlap integral.

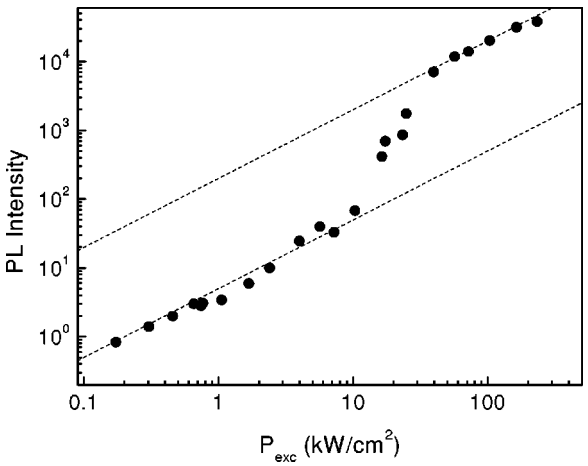

FIG. 2. The dependence of the integrated PL intensity on the laser excitation power P_{exc} for sample *B*.

Below we will consider emission spectra of ZnSe/BeTe structures both at low and high excitation regimes.

B. Low excitation regime

1. Structure with equivalent Te-Zn$\cdots$Zn-Te interfaces

The emission at normal and inverted interfaces in the structure with equivalent interfaces has opposite dominating linear polarization due to a mutually perpendicular direction of the interface bonds. At zero electric field across the structure the transition energies at two interfaces are equal to each other and no linear polarization of emission is expected due to an equal transition probability at the interfaces. The electric field disturbs the equality of the transition energies and probabilities (namely J^2) at the interfaces. It is clear from Fig. 1(c) that the sign of the energy shift of the emission line with applied electric field allows one to assign the optical transition to the normal or inverted interfaces.

Figure 3 displays linearly polarized time-integrated PL spectra for the sample B with equivalent Te-Zn$\cdots$Zn-Te interfaces at various external voltages in the spectral range of spatially indirect transitions. The spectra are recorded at low photoexcitation density $P_{exc}\approx$10 kW/cm^2 and $T=5$ K. The

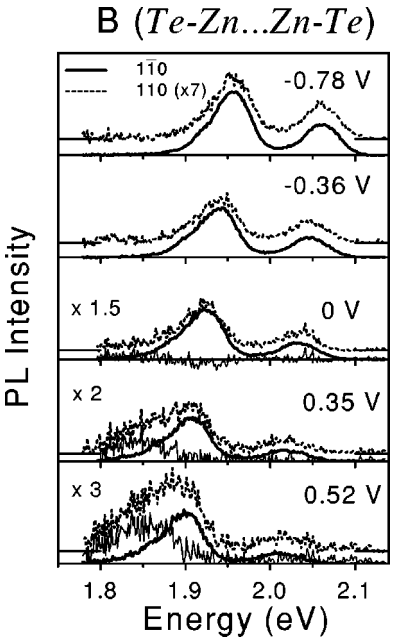

FIG. 3. Linearly polarized time-integrated PL spectra of sample B at low photoexcitation density $P_{exc} \approx 10$ kW/cm^2 and different external voltages (labeled in the figure) at $T=5$ K. Thick solid lines—PL spectra, polarized along the $[1\bar{1}0]$ principal axis, dotted lines—along [110] axis (multiplied by a factor of 7 and shifted vertically for clarity). Thin solid lines—difference of the latter and the former (see text). For the three lower panels the vertical scales are changed by a factor given in the figure.

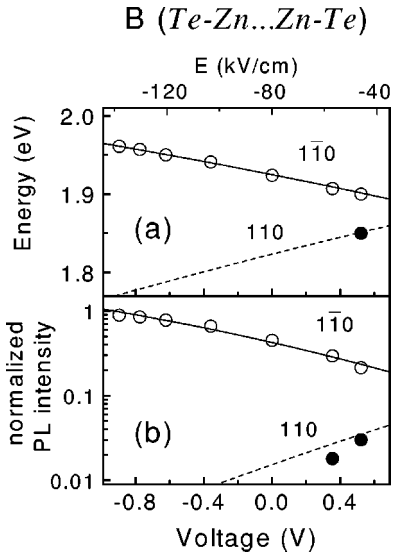

FIG. 4. Experimental (dots) and calculated (lines) dependencies of spectral position (a) and PL intensity in two polarizations (b) for the IT band on external voltage in sample *B*. Low photoexcitation density $P_{exc} \approx 10$ kW/cm^2.

spectral position of the emission at this P_{exc} is shifted to higher energies about 10 meV compared to the low excitation limit.[3,7] As a rule, the observed structure in the spectral range of spatially indirect transitions consists of two bands, the intensity of the violet one being less than that of the band at low energy. This is assumed to result from the radiative recombination of QW's from the top layer and from four lower layers (e.g., due to different mechanical stress). Figure 3 shows that (i) in both polarizations the lines shift linearly to the lower energies, by approximately 45 meV/V, and decrease in the intensity with increasing voltage, (ii) the emission is highly linearly polarized (about 75%) in the whole range of biases and P_l does not change sign in the whole range of *V*, and finally, (iii) the emission spectra in the [110] polarizations multiplied by a factor of 7 coincide well with those in $[1\bar{1}0]$ polarization in a wide range of applied voltages. Only for $V \geqslant 0.3$ V an additional emission appears at the low-energy tail of the [110]-polarized spectrum. A similar behavior (line shift and polarization degree) of two observed lines, corresponding to the spatially indirect transition, with the increasing electric field indicates that they originate from one interface.

The similar emission polarization and monotonic linear line shift in the whole investigated bias range from -0.9 to 0.5 V indicate that the emission dominating the spectrum both at positive and negative voltages originates from the same sort of interfaces. Its assignment is determined from the line shift: The decreasing transition energy is the characteristic for the inverted interface that is Te-Zn in our case. No line with dominating [110] polarization corresponding to the emission from normal interfaces appears up to $V=0.5$ V. Later, in Sec. III B, we will show that the inclusion of the regions with Be-Se bonds at the Zn-Te interface is relatively small. Thereby one has to suppose that the external field is not enough to overcompensate the field caused by a built-in voltage $V_{in} \approx -0.6$ V from the the Schottky barrier at the Au contact[16] and shift the electrons and holes to this interface. However, Fig. 3 shows that the marked difference in the line shape recorded in two crossed polarizations appears near $V=0.5$ V. An additional contribution shows up in [110] polarized spectra at the low energy tail of the emission line at 1.85 eV. Based on its polarization it is naturally to assign this contribution to the recombination at normal interfaces. That means that the transition energy at the normal interface is smaller than that at the inverted one and proves that the electric field does not change the sign up to maximum used voltage of $V=+0.5$ V ($V_{in}+V<0$).

At the negative voltages, the emission from the normal interface is completely negligible, the ratio of PL intensities in the two linear polarizations $I_{1\bar{1}0}:I_{110}=7:1$ is just equal to the ratio of matrix elements $\alpha_n = p^2_{1\bar{1}0}/p^2_{110}$ for transitions in the two polarizations at the Te-Zn interface. For the opposite, Zn-Te, interface, with Zn-Te bonds rotated by 90 deg, the ratio $p^2_{1\bar{1}0}/p^2_{110}$ is just inverted, resulting in $\alpha_i = 1/7$. The line shape of the contribution from the inverted layer at positive *V* can be extracted with the use of Eqs. (1) and (2) by substituting $\alpha_n = 7$ and $\alpha_i = 1/7$. Figure 3 shows this contribution at 0.35 V and 0.52 V with thin solid lines. In the latter case, the emission band is well observable. It is located about 50 meV below that from the direct interface (thick solid line) and has the intensity about an order of magnitude smaller.

The measured transition energies and emission intensities at normal and inverted interfaces with bias are shown in Fig. 4 by solid and open dots, respectively. The solid and dashed

lines are the fitting of experimental bias dependencies by calculated ones. The calculated dependencies have been obtained by solving the self-consistent problem of the coupled system of Schrödinger and Poisson differential equations.[2,3,20] No renormalization effects due to many-body Coulomb interaction have been taken into account. This approximation is justified for a semiquantitative description of a dense electron-hole system when the Fermi energy strongly exceeds the exchange-correlation energy.[21–23] The fitting to the experimental data has been achieved by scaling the voltage to the electric field to get the total line shift in the $[1\bar{1}0]$ polarization. According to this scaling, the obtained range of electric fields[24] is from -135 to -45 kV/cm with an accuracy of ± 10 kV/cm. The line intensities are fitted by calculating the dependence of the squared electron-hole integral. Figure 4 shows that calculations of the overlap integral in this range of -135 to -45 kV/cm gives a four-fold decrease in the line intensity, which is in a good agreement with the change in the PL intensity from the inverted Te-Zn interface shown in Fig. 4(b). Also the relative emission intensity from the normal Zn-Te interface observed at $V=0.5$ V is in a reasonable agreement with calculations.

On the other hand, a good agreement between the overlap integral and the change in the PL intensity, which depends on the ratio of τ_r/τ_{nr} at $\tau_r \gg \tau_{nr}$ shows that τ_{nr} remains independent of the shape of wavefunction at different electric fields. That in turn indicates that the spatial distribution of nonradiative centers is homogeneous.

2. Structures with nonequivalent Te-Zn···Se-Be interfaces

In the structure *A* the Te-Zn and Se-Be bonds at opposite interfaces are parallel resulting in the same sign of their emission polarization. Therefore the polarization cannot be used as a criterion for assignment of the line to specific interfaces. In this case the emission lines of direct and inverted interfaces can be distinguished only when they are separated spectrally at high sufficient electric fields, Fig. 5 displays linearly polarized, time-integrated PL spectra for the sample *A* recorded at $P_{exc} \approx$ 10 kW/cm^2 and various external voltages. The emission is highly linearly polarized in the whole range of biases, the polarization degree is as high as 75% in a very broad range of *V* and decreases slightly to 62% only at maximum positive voltages. The 75% polarization degree is the characteristic for the Te-Zn interface that is the inverted interface in the sample *A* as well as in the sample *B*. The fact that the dominating emission corresponds to the Te-Zn inverted interface also at positive *V* is confirmed by a monotonic, nearly linear line shift to lower energies and a decrease in its intensity with increasing *V*. The line from the normal interface should show the opposite dependencies. Moreover, the lineshift and the change in its intensity just coincide with those for the inverted Te-Zn interface in the sample *B*. The absence of a marked emission from the normal Se-Be interface can be explained by a much smaller electron-hole overlap at the normal interface (the total electric field across the heterostructure is negative even at $V \sim 0.5V$ due to an Au contact induced additional built-in electric field) or by a much smaller transition probability at Se-Be interfaces compared to Te-Zn interfaces. We will discuss this question in the following section.

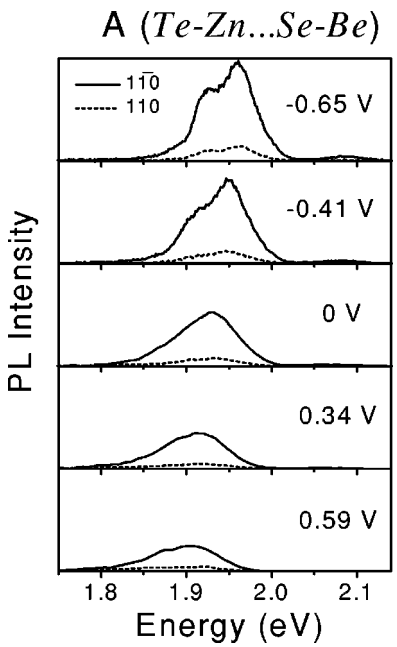

FIG. 5. Linearly polarized time-integrated PL spectra of sample *A* at low photoexcitation density $P_{exc} \approx 10$ kW/cm^2 and different external voltages (labeled in the figure) at $T=5$ K. PL spectra, polarized along the $[1\bar{1}0]$ and [110] principal axes, are shown by solid and dotted lines, respectively.

C. High excitation regime

1. Structure with equivalent Te-Zn···Zn-Te interfaces

Let us now consider modifications in the type-II interface emission with increasing excitation density. Figure 6 shows the time-integrated PL spectra for sample *B* in both polarizations at different external voltages. The spectra were recorded at $P_{exc} \approx 50$ kW/cm^2 and $T=5$ K. The higher density of spatially separated electrons and holes in the ZnSe and BeTe layers realized under this photoexcitation level results in an additional band bending and a blue shift of the IT band maximum.[3] The line maximum is located at ~ 2.08 eV. Numerical calculations[3] show that this value corresponds to densities of spatially separated electrons and holes of about 2×10^{12} cm^{-2}. In addition, the increase in carrier density leads to a marked line broadening due to the increasing quasi-Fermi energies for electrons and holes.[4] One can see from Fig. 6 that the IT linewidth at $P_{exc} \approx 50$ kW/cm^2 exceeds 200 meV.

Comparison of Figs. 6 and 3 shows that both the polarization degree and the spectral shift of the IT band in the interval $-0.9 < V < +0.6$ V decrease drastically. Particularly, the spectral shift decreases from 45 meV/V at low P_{exc} to less than 10 meV/V at high P_{exc}. The IT emission band shift at $P_{exc} \approx 50$ kW/cm^2 is displayed in Fig. 7. Here the center of gravity of the IT emission band is used as its spectral position because the line half-width exceeds markedly its

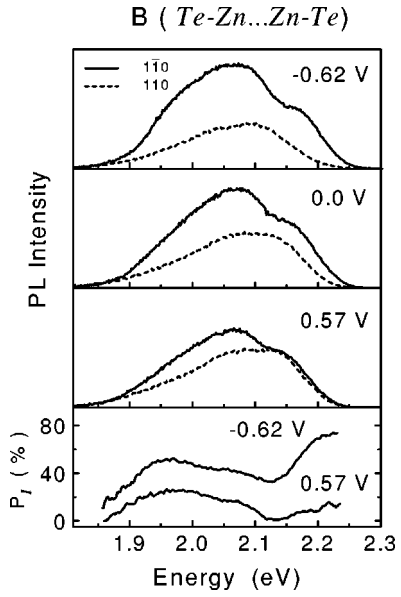

FIG. 6. Linearly polarized time-integrated PL spectra of sample *B* at different applied voltages (labeled in the figure) at high photoexcitation density $P_{exc} \approx 50$ kW/cm^2. At the bottom row are given the spectral dependencies of the polarization degree P_l. $T=5$ K.

shift. First, it is seen that the $[1\bar{1}0]$-polarized line shifts to lower energies whereas the [110]-polarized line shifts to higher energies. This behavior allows us to conclude that these lines originate from opposite interfaces. Second, in contrast to the case of low excitation level, the ratio of intensities in the two polarizations varies with V in the whole range from -0.6 to 0.6 V . More precise information is obtained from the spectral dependence of $P_l(\hbar\omega)$ in Fig. 6. The emission from the inverted Te-Zn interface at $V=-0.6$ V is essentially redshifted leaving the violet range for the emission from the only Te-Zn normal interface. Figure 6(c) shows that P_l as high as $\approx 75\%$ is observed at $\hbar\omega = 2.2$–2.25 eV. A fast decrease of P_l at smaller $\hbar\omega$ is connected with the appearing contribution from the opposite interface. P_l of 75% at the high-energy side of the emission spectrum corresponds to the emission of high-energy carriers. Nevertheless this polarization degree just coincides with that measured at the low-density excitation level. Thus we can conclude that the ratio of matrix elements in the two polarizations is nearly independent of carrier energy. This result is in agreement with experiments reported in Ref. 12 and theoretical calculations of Ivchenko *et al* who found that the polarization degree of the emission at the interface depends on carrier energy very weakly.[19]

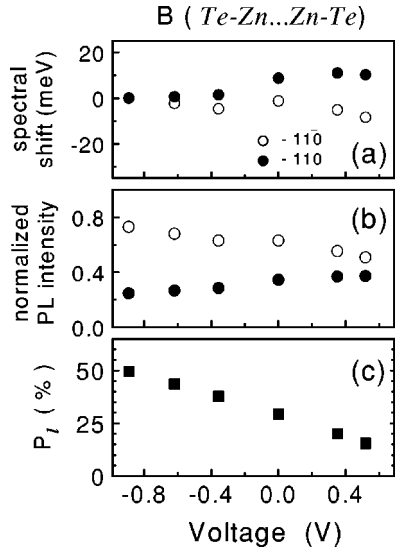

FIG. 7. Spectral characteristics of the IT band vs external voltage in sample *B* : (a) spectral shift relative to the position at the minimal external voltage used in experiment, (b) normalized intensity in both polarizations and (c) spectrally integrated polarization degree P_l. High photoexcitation density $P_{exc} \approx 50$ kW/cm^2 and $T=5$ K.

Figs. 7(a) and 7(b) display the shift of the emission lines and their intensities at two interfaces on bias voltage at the high excitation density. Figure 7(a) shows that $dE_{IT,n}/dV$ is less than 10 meV/V. A strong decrease of $dE_{IT,n}/dV$ compared to the low excitation level (~ 45 meV/V, Fig. 4) indicates that the external voltage across the ZnSe/BeTe heterostructure decreases drastically with increasing carrier density. Note that our experiments show that any effect of an external voltage on the luminescence spectrum disappears, with increasing P_{exc} to 500 kW/cm^2. A comparison with calculations shows that at $P_{exc} \approx 50$ kW/cm^2 the difference in the electric field $\Delta E = E(-0.9\text{V}) - E(+0.5\text{V})$ is equal to 15–20 kV/cm. Such a change in the electric field results in a relatively small redistribution of electron and hole wave functions across the quantum well. The respective changes in the emission intensity should not exceed a factor of 2. The latter is in a good agreement with experimental data given in Fig. 7(b).

The other important distinction of the results at $P_{exc} \approx 50$ kW/cm^2 from those at low photoexcitation powers is that the sum of the PL intensities of the IT bands in different polarizations remains approximately constant and independent of the external voltage as can be seen from Fig. 7(b). These data indicate that at high excitation powers nonradiative recombination processes are saturated and the observed PL is determined by radiative lifetime τ_r. The externally applied electric field provides a possibility to control τ_r at the normal and inverted interfaces and thus to govern the polarization degree of the IT band in the symmetrical heterostructure.

2. Structures with nonequivalent Te-Zn···Se-Be interfaces

The linearly polarized emission spectra in two polarizations and $P_l(\hbar\omega)$ at various applied voltages for the sample *A* with Te-Zn$\cdots$Se-Be interfaces configuration are displayed in Fig. 8. As expected for this sample with identically oriented chemical bonds at two interfaces the emission intensity in the $[1\bar{1}0]$ direction exceeds strongly that in the [110] direction in the whole range of used voltages. With increasing electric field from -0.7 to $+0.6$ V, the $[1\bar{1}0]$-polarized line shifts to lower energies by about 10 meV (which is similar to that for the sample B at the same excitation density) and decreases in intensity [see Fig. 8(a)]. Both appear-

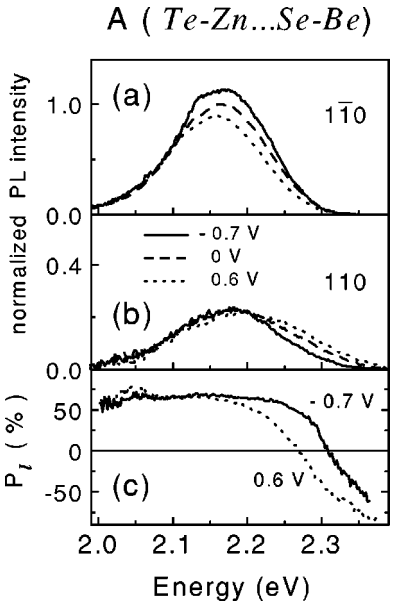

FIG. 8. Linearly polarized time-resolved PL spectra in the $[1\bar{1}0]$ polarization (a), [110] polarization (b), and the corresponding polarization degree vs spectral position (c) of sample *A* at different external voltages (labeled in the figure). $P_{exc} \approx 50$ kW/cm^2 and $T=5$ K.

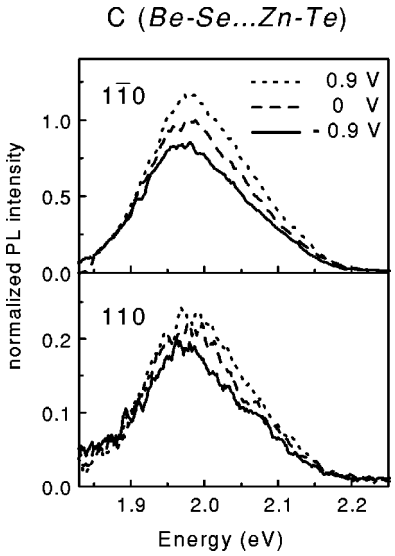

FIG. 9. Linearly polarized time-integrated PL spectra in the $[1\bar{1}0]$ polarization (a) and [110] polarization (b) of sample *C* at different external voltages (labeled in the figure). $P_{exc} \approx 100$ kW/cm^2 and $T=5$ K.

ances indicate that the dominant emission originates from the inverted Te-Zn interface. Unexpectedly, Fig. 8(b) shows that the IT band in the [110] polarization broadens and its violet edge shifts to the higher-energy side with increasing voltage. As a result, P_l reaches -70$\pm$10% at the violet edge at positive voltages. Note that this polarization value cannot be connected with emission from the areas with Se-Be bonds at the normal interface because these bonds have the same orientation as the Te-Zn bonds at the inverted interface and have to provide the same polarization. The negative sign of polarization on the violet edge of the IT band at $V=0.6$ V indicates that this emission occurs at minor inclusions of Zn-Te interface in the primarily Se-Be normal interfaces. This assignment is also supported by the fact that $|P_l|$ at $V=0.6$ V at two sides of emission spectra coincide with each other and within an experimental error are equal to $|P_l|$ at the Te-Zn interface ($\approx$75%). Note once more that the emission from the areas with Se-Be bonds at the normal, mainly Se-Be interface has the $[1\bar{1}0]$ polarization. Thereby any marked contribution of emission from this areas has to result in a decrease of the polarization degree below 75%. The absence of any pronounced emission from the areas with Se-Be bonds can be explained if we accept that the squared matrix element for this transition is more than one order of magnitude smaller than that for the Te-Zn interface.

We have attempted also to find the emission from the Be-Se interface in the structure *C* with the inverted Be-Se and normal Zn-Te interfaces, where the built-in electric field caused by the Au contact shifts the carriers to the Be-Se interface. The experimental problem with this structure is in its very low quantum efficiency.[13] To excite a dense electron-hole gas, $P_{exc}=100$kW/cm^2 has been used. Figure 9 displays the polarized spectra from this sample in the range of *V* from -0.9 to $+0.9$ V. This figure shows that the emission is highly polarized: the ratio of the intensities in the two polarizations is 6–7 which is similar to that in the sample *A*. To assign the emission in preferred polarization, we have analyzed the line shift with increasing bias. Figure 10 shows that in contrast to the sample *A*, the emission line in the favored polarization along $[1\bar{1}0]$ direction moves in the sample *C* to higher energies. That means that this emission originates from the normal interface that is the Zn-Te one. Thus, again the contribution from the Be-Se interface is negligible even at negative voltages when the electron and hole layers are definitely strongly shifted to the latter interface. Hence no information on the anisotropy of the transition matrix elements at the Be-Se interface can be extracted.

The absence of any observable emission from the Be-Se interface in two samples with direct and inverted Be-Se in-

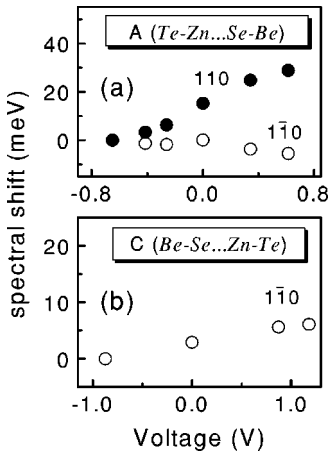

FIG. 10. Shift of the spectral position of the IT band relative to the position at minimal external voltage used in experiment vs external voltage in sample *A* (a) and sample *C* (b).

terface in the whole range of applied voltages indicates, that it has a much smaller optical matrix element than the Zn-Te one. Measurements in the electric field allow to obtain the crude estimation of the maximum possible ratio for p^2 at Se-Be to Te-Zn interfaces in the favored polarization. To explain the absence of the Be-Se-interface emission line in the whole interval of used biases one can take this ratio larger than 1:50. Partially this difference is due to the decreased tunneling of electrons and holes into the neighboring layers at Be-Se interface originating from a larger band gap of the virtual (1 ML thick) ''interface layer'' Se-Be (5.4 eV) compared to the Te-Zn (2.4 eV).[13] However, more detailed calculations in a tight-binding model are necessary to obtain quantitative results.

IV. CONCLUSIONS

The influence of electric fields on the intensity, the spectral shift and the in-plane polarization anisotropy of spatially indirect radiative recombination in type-II ZnSe/BeTe heterostructures with equivalent and nonequivalent interfaces is studied in a wide range of P_{exc}. The electric field shifts the wave functions $\Psi_e(z)$ and $\Psi_h(z)$ so that both the overlap integrals and the transition energies for the indirect emission increase at one and decrease at the other interface. As a result contributions to PL from the normal and inverted interfaces can be separated and analyzed.[25]

In the experiment, the effects of the Au contact to the ZnSe layer induced a built-in electric field across the structure which has been taken into account. At low photoexcited carrier densities ($\leqslant 10^{11}$ cm^{-2}), the change of the PL intensity of $\sim$ a factor of 4 and a spectral shift of $\sim$60 meV have been achieved by applying external electric fields to ZnSe/BeTe heterostructures with equivalent (Te-Zn$\cdots$Zn-Te) and nonequivalent (Te-Zn$\cdots$Se-Be) interfaces. The emission from the the Te-Zn interface has been well defined and analyzed. The ratio of matrix elements for optical transitions at the Te-Zn interface,which determines the in-plane optical anisotropy, is equal to $\sqrt{7}$.

At high density of photoexcited carriers of $\sim 10^{12}$ cm^{-2} the changes in the line shift and intensity in the same range of biases are much smaller. However, the polarization studies allow to separate partly the emission from direct and inverted Zn-Te interfaces and to determine the ratio of matrix elements in two polarizations for carriers near the Fermi edge. This ratio is $\sqrt{7}$:1 and turns out to be very similar to the case of low-density photoexcitation. Thus we conclude that the matrix-element anisotropy is nearly independent of carrier density, that is in agreement with theoretical predictions.[19]

Attempts to separate the emission on Be-Se interfaces in heterostructures with nonequivalent Te-Zn$\cdots$Se-Be and Be-Se$\cdots$Zn-Te interfaces were not successful. The emission on primarily Be-Se interfaces has been shown to be masked by that from the small inclusions of Zn-Te areas. An estimate of the ratio of radiative recombination times at Be-Se to Zn-Te interface gives the radiative lifetime at Be-Se interface to be at least 50 times longer than that at Zn-Te interface.

ACKNOWLEDGMENTS

We would like to thank E.L. Ivchenko and N.A. Gippius for useful discussions. The work was supported by the grants from Grant Nos. INTAS 9915, RFBR 01-02-17750, and the Deutsche Forschungsgemeinschaft through Grant Nos. SFB 410.

*Also at A. F. Ioffe Physico-Technical Institute, Russian Academy of Sciences, 194021 St. Peterburg, Russia.

[1] F.C. Zhang, H. Luo, N. Dai, N. Samarth, M. Dobrowolska, and J.K. Furdyna, Phys. Rev. B **47**, 3806 (1993).

[2] W. Langbein, M. Hetterich, and C. Klingshirn, Phys. Rev. B **51**, 9922 (1995).

[3] S.V. Zaitsev, V.D. Kulakovskii, A.A. Maksimov, D.A. Pronin, I.I. Tartakovskii, N.A. Gippius, T. Litz, F. Fisher, A. Waag, D.R. Yakovlev, W. Ossau, and G. Landwehr, JETP Lett. **66**, 376 (1997).

[4] A.A. Maksimov, S.V. Zaitsev, I.I. Tartakovskii, V.D. Kulakovskii, D.R. Yakovlev, W. Ossau, M. Keim, G. Reuscher, A. Waag, and G. Landwehr, Appl. Phys. Lett. **75**, 1231 (1999).

[5] A. Waag, F. Fischer, H.-J. Lugauer, Th. Litz, J. Laubender, U. Lunz, U. Zehnder, W. Ossau, T. Gerhard, M. Möller, and G. Landwehr, J. Appl. Phys. **80**, 792 (1996).

[6] A. Waag, F. Fischer, K. Schull, T. Baron, H.-J. Lugauer, Th. Litz, U. Zehnder, W. Ossau, T. Gerhard, M. Keim, G. Reuscher, and G. Landwehr, Appl. Phys. Lett. **70**, 280 (1997).

[7] A.V. Platonov, D.R. Yakovlev, U. Zehnder, V.P. Kochereshko, W. Ossau, F. Fischer, Th. Litz, A. Waag, and G. Landwehr, J. Cryst. Growth **184/185**, 801 (1998).

[8] A.A. Maksimov, S.V. Zaitsev, I.I. Tartakovskii, V.D. Kulakovskii, N.A. Gippius, D.R. Yakovlev, W. Ossau, G. Reuscher, A. Waag and G. Landwehr, Phys. Status Solidi B **221**, 523 (2000).

[9] M. Schmidt, M. Grün, S. Pettillon, E. Kurtz, and C. Klingshirn, Appl. Phys. Lett. **77**, 85 (2000).

[10] D.R. Yakovlev, A.V. Platonov, V.P. Kochereshko, E.L. Ivchenko, M. Keim, W. Ossau, A. Waag, and G. Landwehr, J. Cryst. Growth **214/215**, 345 (2000).

[11] A.V. Platonov, V.P. Kochereshko, E.L. Ivchenko, D.R. Yakovlev, M. Keim, W. Ossau, A. Waag, and G. Landwehr, Phys. Rev. Lett. **83**, 3546 (1999).

[12] D.R. Yakovlev, E.L. Ivchenko, V.P. Kochereshko, A.V. Platonov, S.V. Zaitsev, A.A. Maksimov, I.I. Tartakovskii, V.D. Kulakovskii, W. Ossau, M. Keim, A. Waag, and G. Landwehr, Phys. Rev. B **61**, R2421 (2000).

[13] S.V. Zaitsev, A.A. Maksimov, V.D. Kulakovskii, I.I. Tartakovskii, D.R. Yakovlev, W. Ossau, L. Hansen, G. Landwehr, and A. Waag, J. Appl. Phys. **91**, 652 (2002)

[14] T. Walter, A. Rosenauer, R. Wittmann, D. Gerthsen, F. Fischer, T. Gerhard, A. Waag, G. Landwehr, P. Schunk, and T. Schimmel, Phys. Rev. B **59**, 8114 (1999).

[15] M. Nagelstraßer, H. Dröge, H.-P. Steinrück, F. Fisher, T. Litz, A. Waag, G. Landwehr, A. Fleszar, and W. Hanke, Phys. Rev. B **58**, 10 394 (1998).

[16] V. Wagner, M. Becker, M. Weber, T. Füller, M. Korn, and J.Geurts, Thin Solid Films **364**, 119 (2000).

[17] A.A. Maksimov, S.V. Zaitsev, I.I. Tartakovskii, V.D. Kulakovskii, D.R. Yakovlev, W. Ossau, M. Keim, G. Reuscher, A. Waag, and G. Landwehr, in *Proceedings of the ICPS25*, edited by N. Miura and T. Ando, (Springer, Berlin, 2001) p. 637.

[18] A.A. Maksimov, S.V. Zaitsev, I.I. Tartakovskii, V.D. Kulakovskii, D.R. Yakovlev, W. Ossau, M. Keim, G. Reuscher, A. Waag, and G. Landwehr (unpublished).

[19] E.L. Ivchenko and M.O. Nestoklon, ZETP (to be published).

[20] P. Ruden and G.H. Döhler, Phys. Rev. B **27**, 3538 (1983).

[21] N.A. Gippius, S.G. Tikhodeev, M. Bayer, in *Proceedings of 23rd International Conference on Physics of Semiconductors*, edited by M. Scheffler and R. Zimmermann, (World Scientific, Singapore 1996), Vol. 3 p. 2075.

[22] G. Träkle, T. Lach, A. Forchel *et al.*, Phys. Rev. Lett. **58**, 419 (1987).

[23] V.D. Kulakovskii, E. Lach, A. Forchel, and D. Grützmacher, Phys. Rev. B **40**, 8087 (1989).

[24] This range is approximately two times smaller than calculated one as V/d where d is the structure thickness. The difference is connected with the fact that a significant part of voltage drops at the contacts, most probably, at the ZnSe/Au contact.

[25] A.A. Maksimov, S.V. Zaitsev, P.S. Dorozhkin, V.D. Kulakovskii, I.I. Tartakovskii, N.A. Gippius, D.R. Yakovlev, W. Ossau, L. Hansen, G. Landwehr, and A. Waag, Phys. Status Solidi B **229**, 35 (2002).